

EXPERIMENTAL INVESTIGATION ON REAL-TIME REMOTE SENSING OF LAYERED ATMOSPHERIC PRECIPITABLE BY A GROUND-BASED RADIOMETER OF 1.35 cm WAVELENGTH*

Huang Runheng (黄润恒) and Wei Chong (魏 重)

Institute of Atmospheric Physics, Academia Sinica, Beijing

Received April 11, 1985

ABSTRACT

The principle and technique of real-time remote sensing of the layered atmospheric precipitable by using a ground-based radiometer of 1.35 cm wavelength with a microcomputer as a controlling and data processing unit are presented. The stability and calibration of the instrument are outlined. Observations during the summer of 1984 show that the RMS deviation of the layered precipitable between the radiometer measurement and the radiosonde ranges from 0.20 to 0.25 g/cm² with a correlation coefficient of above 90 %.

1. INTRODUCTION

The atmospheric water is one of the most vigorous factors in a variety of weather phenomena. The knowledge about the spatial structure, temporal evolution of water vapor as well as its phase transition is of virtual importance to the short-term weather prediction and the nowcasting. Moreover, the atmospheric water vapor content (WVC) is an indispensable factor for the atmospheric correction in the astronomical observation, the microwave propagation and the remote sensing. Contemporary scientists all over the world have paid much attention to monitoring the water vapor variation by means of the passive microwave technique^[1-3]. The WPL/NOAA (the Wave Propagation Laboratory/National Oceanic and Atmospheric Administration of U.S.A) have put this radiometer for water vapor remote sensing into the profiler system which belongs to the proto regional observation and forecasting service (PROFS)^[4]. In 1982 we successively measured the atmospheric total precipitable by using a ground-based radiometer developed by ourselves. Meanwhile, we made an experiment of retrieving the vertical profile of water vapor in terms of so-called "Monte Carlo method"^[5]. It provides a possibility to continuously monitor the temporal evolution of water vapor field. However, the Monte Carlo method requires a medium-size computer with a consuming computer time, while a single parameter of the total precipitable is not able to reflect the spatial structure of water vapor field. In order to remedy these two disadvantages we used the radiometer with a microcomputer as a controlling and data-processing unit^[6] to make an experiment continuously and to real-timely obtain the layered atmospheric precipitable.

* Ma Changwang, Chen Ying, Zhu Xiaomin of IAP and Zhang Ming of Beijing Meteorological Bureau took part in observations.

Outlined in this paper are the principle of real-time remote sensing of layered WVC, the calibration of the radiometer system as well as the experimental results.

II. THE MEASUREMENT PRINCIPLE

The principle of atmospheric microwave remote sensing was extensively discussed everywhere (for example, see Ref. [7]). The basic concept to extract the desired atmospheric parameters from the measured atmospheric brightness temperature is through the equation

$$T_{B_V}(\theta) = T_{B_g} \exp \left[- \int_0^{\infty} \alpha_v(z) \sec \theta dz \right] + \int_0^{\infty} T(z) \alpha_v(z) \exp \left[- \sec \theta \int_0^z \alpha_v(z') dz' \right] \sec \theta dz, \quad (1)$$

where T_{B_g} is the cosmic background microwave brightness temperature, θ the zenith angle, $T(z)$ the atmospheric temperature profile, α_v the atmospheric microwave absorption coefficient which mainly depends on the microwave absorption constituents in the atmosphere. It shows that the microwave radiation received by a radiometer is the weighted summation of atmospheric emission, in which $\alpha_v \exp \left[- \sec \theta \int_0^z \alpha_v(z') dz' \right]$ is the weighting function.

Roughly speaking, the microwave radiation of different zenith angles comes mainly from the atmospheric microwave emission below a certain layer. Based on the quantitatively analysis we can develop a correspondent relationship between WVC in different heights and brightness temperatures at different zenith angles. Referring to the requirement of the common numerical prediction model, we divide the atmosphere into four layers, i. e., 1000—850 hPa, 1000—700 hPa, 1000—500 hPa and total layer. The observation elevation angles are taken to be 10, 12, 15, 18, 20, 25, 30, 40, 60, 90 degrees. The numerical experiment shows that a multi-regression relationship exists between layered WVC and brightness temperatures,

$$Q = Q_0 + C_1 \cdot (T_B - T_{B_0}), \quad (2)$$

where Q represents four-dimensional vector of layered precipitable, T_B ten-dimensional observation vector of brightness temperature, Q_0 and T_{B_0} their mean vectors, respectively, C_1 is the regression coefficient matrix. By selecting the representative sample of clear-air and calculating the brightness temperature and layered WVC from radiosonde data, the coefficient matrix C_1 can be obtained by means of the standard statistical regression technique. Shown in Table 1 is the numerical result for the 26 radiosonde samples of July—August, 1984.

Table 1. The Statistics of Regressed Layered WVC from the Calculated Brightness Temperature

Atmospheric Layer	1000-850 hPa	1000-700 hPa	1000-500 hPa	Total Layer	Mean RMS
The Mean Value of Layered WVC (g/cm ²)	1.920	3.181	3.902	4.182	
RMS of Regression (g/cm ²)	0.146	0.188	0.172	0.081	0.152
Correlation Coefficient	0.86	0.92	0.96	0.99	

If a single-parameter regression is taken between the total precipitable and the brightness temperature at the zenithal direction, the RMS deviation is 0.071 g/cm^2 . In comparison with the single-parameter regression, the value shown in Table I reveals a decreased regression accuracy in the multi-regression case, this is due to its making use of the low elevation measurements at which the slant atmospheric attenuation is rather large. Even so, the relative error theoretically is only 2 %.

III. THE MEASUREMENT EQUIPMENT

An impulse noise-input null-balanced Dicke type radiometer developed in our own laboratory was employed in the experiment. The central frequency of the radiometer is 22.235 GHz with a IF band width of 100 MHz. The details of radiometer system is referred to Ref. [8]. The data acquisition and processing of this experiment are different from those conducted in 1982. The frequency/voltage converter transforms the impulse repetition frequency from the impulse generator into a voltage, which is sampled, stored and averaged by the microcomputer. A mean measurement voltage and its RMS fluctuation are output and printed after 240 instantaneous measurement voltages are averaged. The sampling dynamic range of microcomputer is 5 V with a sampling accuracy of 0.02 V. Moreover, the computer controls the observation angle and the scanning of antenna according to the programme preset in. After a complete cycle of observation angle is finished, the microcomputer controls the antenna back to its original position and real-time calculates the brightness temperature of various zenith angles and the desired atmospheric parameters according to the calibration coefficients. When the antenna resets, the radiometer is waiting for the next starting command. Thus, the automatic observation and data processing are realized by the measurement-controlling programme in the microcomputer. In order to monitor the current state of the radiometer system, the inject impulse frequencies are manually printed for the purpose of comparison.

IV. THE RADIOMETER CALIBRATION

The difficulty in the absolute calibration of a radiometer system including an antenna lies in the shortage of the standard microwave radiation source with enough dynamic range. In addition, there is certainly a difference in the response characteristics between the radiometers with and without the antenna reflector. Only a standard low-temperature terminal load (liquid nitrogen) was regularly used to monitor the state of radiometer during the entire experiment. It is expected to evaluate the stability of the radiometer quantitatively. Depicted in Fig. 1 is the diagram of the standard low-temperature source. The output temperature is 82 K with an accuracy of 1 K. Fig. 2 shows some monitoring results continuously lasting a few hours. It can be seen that the RMS fluctuation of the radiometer output is about 0.02—0.06 V. On the basis of the relationship between the radiometer output under the clear-air condition and the calculated brightness temperature from the simultaneous radiosonde profile (see Fig. 3), it concludes that the voltage fluctuation shown above roughly corresponds to a temperature variation ranging 1—3 K. The day-to-day fluctuation is about 0.5 K for four cases in July and larger than 10 K for three continuous records in August. Because the radiometer can not keep stationary during a day while there appears day-by-day fluctuation, we believe that the large fluctuation in August is due to the inadequate use of the low-temperature terminal load.

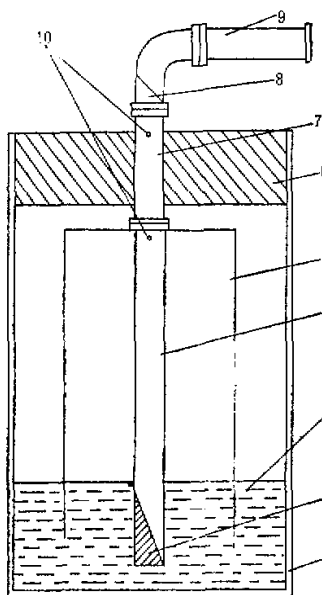


Fig. 1. The diagram of the low-temperature terminal load: (1) Dewar vacuum flask, (2) matched terminal, (3) liquid nitrogen, (4) copper waveguide, (5) nitrogen gas collector, (6) polyvinyl phenyl cover, (7) stainless steel waveguide, (8) foam plastic window, (9) room-temperature waveguide, and (10) cycle hole.

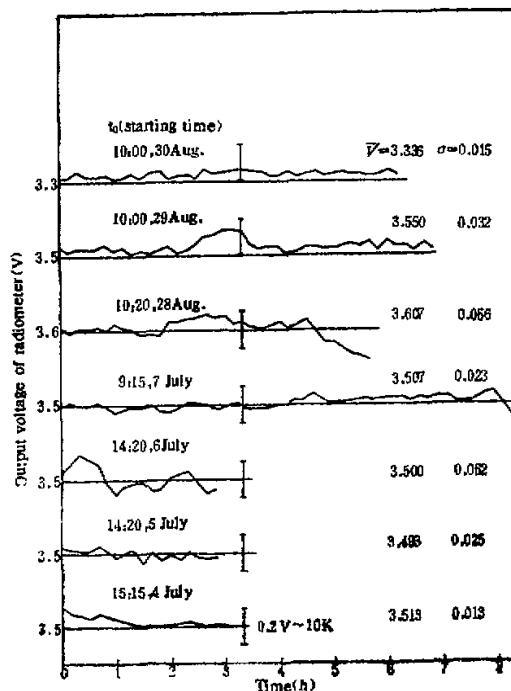


Fig. 2. The continuous output voltage of the radiometer with a standard low-temperature terminal load. t_0 is the starting time, and V the averaged output voltage with the deviation σ .

Shown in Fig. 3 are several examples of measurements in the real atmosphere. They illustrate that there is a correspondent relationship between the radiometer output voltage at different elevation angles and the calculated brightness temperature from the simultaneous radiosonde data. This relationship may be approximate with a linear one, of which the slope is about 50 K/V. On the other hand, the correspondence among the data is rather scatter, some appear systematically translated. The RMS error may approach to 10 K if a single voltage calibration procedure is adopted. But, regarding to the effect of the antenna side-lobe, the brightness temperature at a particular elevation angle is also dependent on the atmospheric emission at other angles. A reasonable choice here is to use the multi-regression technique between the brightness temperature and the output voltage at a series of elevation angles. Thus

$$T_B = T_{B0} + C_2 \cdot (V - V_0), \quad (3)$$

where V is the observation voltage vector, V_0 its mean vector, and C_2 the multiregression matrix. Shown in Table 2 are the calibration results for some elevation angles. A comparison between the calibrated and calculated brightness temperatures is given in Fig. 4.

Table 2. The "Natural" Calibration Results of the Radiometer

Elevation Angle	10	20	40	90	Mean RMS
RMS of Statistical Regression (K)	6.5	6.0	5.0	3.1	5.4
Correlation Coefficient	0.96	0.97	0.97	0.97	

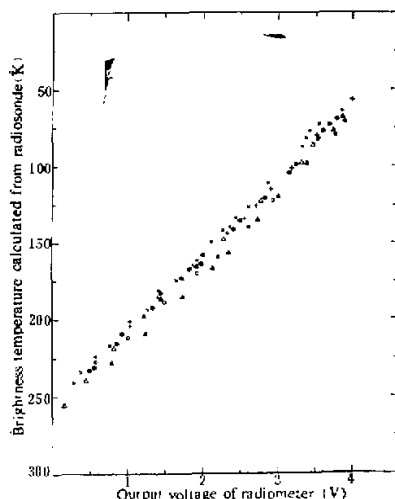


Fig. 3. Examples of the radiometric measurement. Different symbols represent different measurements of zenith angle scanning.

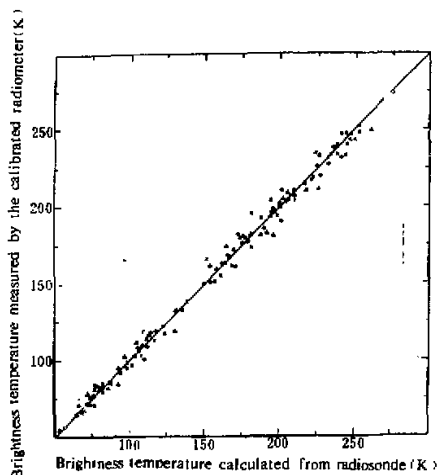


Fig. 4. A Comparison of the calibrated brightness temperature to that calculated from the simultaneous radiosonde data.

In order to partly avoid the calibration error in brightness temperature, which comes from the measurement error as well as the modeling error, we developed a direct relationship between the output voltages and the layered WVC integrated from the radiosonde data as the resultant calibration coefficient matrix for real-time retrieval, i. e.

$$Q = Q_0 + C \cdot (V - V_0). \quad (4)$$

From Eqs. (2) and (3) it can be seen, theoretically

$$C = C_1 \cdot C_2. \quad (5)$$

Entered in Table 3 is the results of radiometrically measured layered precipitable regressed from the 26 set observations.

Table 3. A Comparison of Radiometrically Measured WVC to That of Radiosonde.

Layer	1000-850 hPa	1000-700 hPa	1000-500 hPa	Total Layer	Mean RMS
RMS of Regression (g/cm ²)	0.138	0.203	0.192	0.231	0.194
Correlation Coefficient	0.87	0.91	0.96	0.96	

A comparison of the results in Table 1 to that in Table 3 shows a good consistency in the correlation, while the RMS error in the measurement is larger than that in the numerical experiments. The former includes both measurement and modeling errors, but the latter only modeling error. Because of the mutual independence of both the errors it can be estimated that the RMS error attributed to the measurement is $\sqrt{(0.192)^2 - (0.152)^2} = 0.117$ (g/cm²). Shown in Fig. 5 is a comparison of the layered precipitable measured by the radiometer to that by radiosonde.

V. THE MEASUREMENT RESULTS

As soon as the calibration regression matrix was determined, the layered precipitable can be real-time obtained from the measurement voltages by the microcomputer programme. As a preliminary experiment, a series of daytime measurement continuously lasting for three months in the summer of 1984 were conducted. Except for accident causes, such as power supply and air-conditioning, the observation data including all the fair-weather and cloudy air with Ac and Ci were obtained. From these data 27 samples and 26 samples are selected for the purpose of natural calibration for June-July and for July-August, respectively¹⁾.

Depicted in Fig. 6 is a comparison of the layered WVC measured by the radiometer to that of simultaneous radiosonde. Including the calculation samples, the RMS deviations of four layers are 0.201, 0.220, 0.221, 0.248 g/cm² with correlation coefficient of 0.91, 0.96, 0.98 and 0.97, respectively. Regarding to the inherent difference in the radiometric and radiosonde measurements, the former is a weighted mean of path precipitable water, while the latter is an instantaneous measurement in situ during the balloon ascending, it is understandable for the rather large RMS deviation between them.

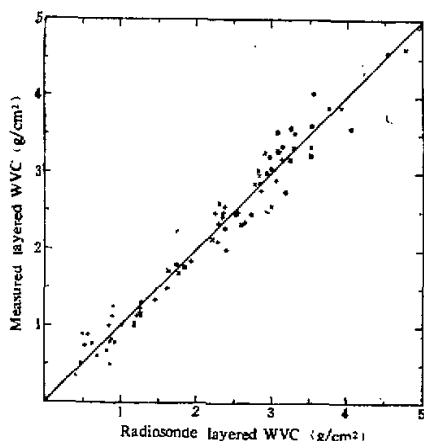


Fig. 5. The calibration samples of radiometrically measured layered WVC. Symbols \cdot , $+$, \times , \circ represent the WVC of 1000-850, 1000-700, 1000-500 hPa and total layer, respectively.

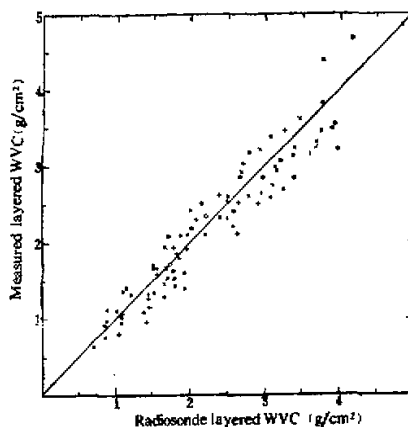


Fig. 6. As in Fig. 5, except for the test sample.

- 1) A new model of microcomputer substituted for the original one in the third of July. Respective natural calibrations before and after that time have to be made in view of the inconsistency in the data.

Fig. 7 shows the temporal evolution of a few continuous measurements. For the purpose of explicitness, shown in this figure are only two layers of precipitable water: the lowest layer (1000–850 hPa) and the total layer. The dots and circles in the figure represent the radiosonde measurements. It can be seen that the general tendency of both measurements is quite consistent though some significant discrepancies exist in particular cases. Another

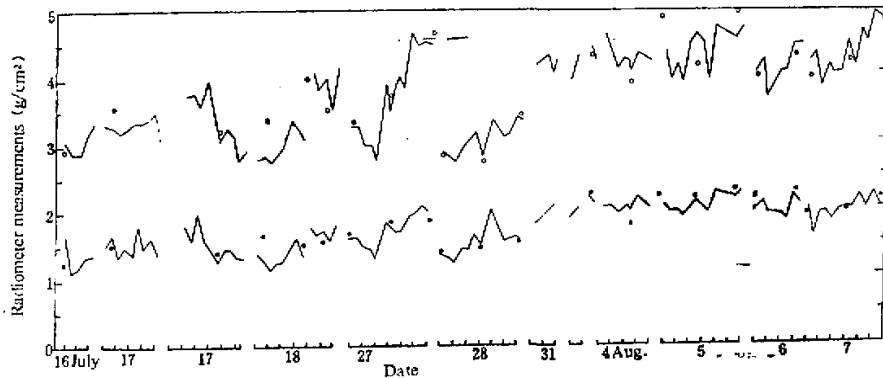


Fig. 7. The temporal variation of layered WVC. One unit in abscissa represents two hr interval.

noticeable characteristic is that the temporal evolution of water vapor field appears to be largely fluctuating for the radiometric measurements. In order to verify whether these fluctuations are meaningful, a numerical simulation was used to analyze the sensibility of inversion coefficient matrix C to the observation error. Assuming that there is a random error vector E in the observation vector, it follows from Eq. (4) that the response of regressed water vapor to the E is

$$\Delta Q = C \cdot E. \quad (6)$$

Experimentally, the RMS error in a single sampling is generally less than 0.1 V, it is derived from the statistical estimation principle for the random sampling^[9] that the RMS error in n samplings is not beyond $0.1/\sqrt{n} = 0.006$ V, where $n=240$. Thus, the microcomputer generates a great number of ten-dimensional random Gaussian vectors, $N(0, 0.006)$, as the random error in the observation vector. Substituting E into Eq. (6), a mean value of ΔQ is derived to be 0.03, 0.05, 0.07 and 0.08 g/cm². It shows that the inversion error due to the observation error through the coefficient matrix is much less than the magnitude of fluctuations in Fig. 7. These fluctuations with time can not be displayed in the radiosonde sequence twice (or four times) a day. It concludes that the radiometer can remotely sense the temporal evolution, fluctuation of water vapor as well as the relationship between the upper and lower atmospheres. How to apply these new information to the weather forecasting and/or other disciplines is an open issue to merit further investigation.

VI. CONCLUSIONS

The elevation scanning radiometer of 1.35 cm wavelength which has a microcomputer as the controlling and data-processing unit can provide a real-time measurement of the layered

WVC. This kind of radiometer is capable of exploring the temporal evolution and the coupling between upper and lower layers of water vapor field. A comparison of radiometric measurement to the radiosonde measurement shows a good consistency in the tendency. Meanwhile the radiometric measurements reveal the significant fluctuation in the temporal variation of water vapor field. Such fluctuation was also displayed by Guiraud et al.^[2] in their measurement chart of 3 hr interval. Ac and Ci clouds have less effect on the microwave measurement for the water vapor. But the influence of the liquid water in the low clouds is not negligible. Moreover, we have conducted a simultaneous observation of 1.35 cm and 8 mm radiometers. These data are helpful to extract the water vapor information under the presence of low clouds.

We would like to thank Zhang Ruizhong, Kang Tianyi, Liu Meijuan and Zhu Jun for designing and developing the microcomputer processing unit. Appreciation is also to Zou Shouxiang for his excellent work in maintenance of the radiometer system.

REFERENCES

- [1] 赵柏林等, 气象学报, 39(1981), 217—225.
- [2] Guiraud, O. et al., *IEEE Trans. on Geoscience Electr.*, GE-17 (1979), p. 129.
- [3] Skoog, B. G. et al., *J. Appl. Meteor.*, 21(1982), 394—400.
- [4] Hogg, D.C. et al., in *Remote Sensing of Atmospheres and Ocean*, Ed. A. Deepak, Academic Press, 1980, 313—364.
- [5] 魏重等, 大气科学, 8(1984), 418—425.
- [6] 郝美娟等, 微机在大气探测中的应用学术交流会议文集, 1984.
- [7] 周秀骥等, 大气微波辐射及遥感原理, 科学出版社, 1982.
- [8] 赵从龙等, 中国科学, B辑, 1983, 8: 759—768.
- [9] J.S. 贝达特等, 随机数据分析方法 (中译本), 国防工业出版社, 1980.